

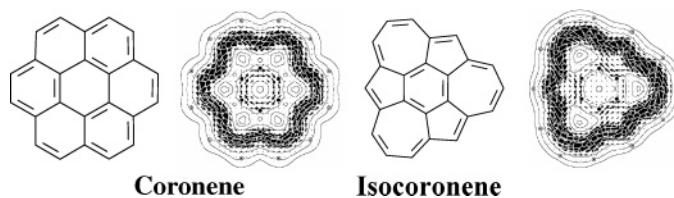
## Super-Delocalized Valence Isomer of Coronene<sup>†</sup>

Arkadiusz Ciesielski,<sup>\*,‡,§</sup> Michał K. Cyrański,<sup>\*,§</sup> Tadeusz M. Krygowski,<sup>§</sup>  
Patrick W. Fowler,<sup>||</sup> and Mark Lillington<sup>||</sup>

Department of Chemistry, University of Warsaw, Pasteura 1, 02–093 Warsaw, Poland, Institute of  
Biochemistry and Biophysics, Polish Academy of Sciences, Pawińskiego 5a, 02–106 Warsaw, Poland, and  
Department of Chemistry, University of Sheffield, Sheffield, S3 7HF, UK

arcad@ibb.waw.pl; chamis@chem.uw.edu.pl

Received April 29, 2006



Coronene (**1**) has been proposed to be “superaromatic”, but energetic, geometric, and magnetic criteria of global and local aromaticity fail to support this proposal, and indeed, the calculated current-density map shows opposition of currents: diatropic on the 18-carbon rim and paratropic on the 6-carbon hub. However, [7,5,7,5,7,5]-isocoronene (**2**) ([7,5,7,5,7,5:6]-circulene, or isocoronene, for short), which is a valence isomer in which alternate pentagons and heptagons replace the hexagons surrounding the central ring, is predicted to have a single, unopposed, intense diatropic perimeter current arising from its four  $\pi$  HOMO electrons, such as in the ipsocentric description of classically aromatic  $[4n + 2]$ -annulenes, hence, qualifying **2** as superaromatic on the magnetic criterion. This conclusion is in excellent agreement with anisotropy of magnetic susceptibility (359 cgs-ppm for isocoronene vs 247 cgs-ppm for coronene) and exaltation of magnetic susceptibility (isocoronene exceeds coronene by 51.4 cgs-ppm). Central and perimeter bond lengths suggest an increased aromaticity of isocoronene. In contrast, the energetic criterion shows that isocoronene is destabilized with respect to coronene by ca. 105 kcal/mol of which only ca. 30 kcal/mol can be attributed to differential strain.

### Introduction

Coronene (**1**) (see Chart 1) is an important benzenoid hydrocarbon, with applications in materials science.<sup>1</sup> This highly symmetric molecule may be viewed as a centrosymmetric model substructure of graphite<sup>2</sup> with distinguishable rim and hub circuits of atoms. Molecular motifs<sup>3</sup> recently have been explored by several groups<sup>4</sup> in work on the magnetic properties of

graphite flakes and their convergence to those of graphite. An intriguing problem, which has attracted much theoretical interest,<sup>5–9</sup> is the possibility of an anticipated enhanced aromaticity (superaromaticity)<sup>10</sup> of coronene’s “ring of rings”.<sup>6</sup>

<sup>†</sup> This paper is dedicated to Professor Janusz Jurczak (Warsaw University and Polish Academy of Sciences) on the occasion of his 65th birthday.

\* Fax: (48) 228–22–28–92; Tel: (48) 228–22–28–92.

<sup>‡</sup> Institute of Biochemistry and BioPhysics, Polish Academy of Sciences.

<sup>§</sup> University of Warsaw.

<sup>||</sup> University of Sheffield.

(1) (a) Yoshimoto, S.; Tsutsumi, E.; Fujii, O.; Narita, R.; Itaya, K. *Chem. Comm.* **2005**, 1188–1190. (b) Kato, T.; Yamaba, T.; *Chem. Phys. Lett.* **2005**, *403*, 113–118. (c) Watson, M. D.; Jäckel, F.; Severin, N.; Rabe, J. P.; Müllen, K. *J. Am. Chem. Soc.* **2004**, *126*, 1402–1407. (d) Chi, X.; Besnard, C.; Thorsmølle, V. K.; Butko, V. Y.; Taylor, A. J.; Siegrist, T.; Ramirez, A. P. *Chem. Mater.* **2004**, *16*, 5751–5755.

(2) Trucano, P.; Chen, R. *Nature* **1975**, *258*, 136–137.

(3) (a) Stein, S. E.; Brown, R. L. *Carbon* **1985**, *23*, 105–109. (b) Stein, S. E.; Brown, R. L. In *Molecular Structure and Energetics*; Liebman, J. F., Greenberg, A., Eds.; VCH: Weinheim, Germany, **1987**; Vol. 2, pp 37–66. (c) Stein, S. E.; Brown, R. L. *J. Am. Chem. Soc.* **1987**, *109*, 3721–3729.

(4) (a) Moran, D.; Stahl, F.; Schaefer, H. F., III; Schleyer, P. v. R. *J. Am. Chem. Soc.* **2003**, *125*, 6746–6752. (b) Soncini, A.; Steiner, E.; Fowler, P. W.; Havenith, R. W. A.; Jenneskens, L. W. *Chem.–Eur. J.* **2003**, *9*, 2974–2981. (c) Geuenich, D.; Hess, K.; Köhler, F.; Herges, R. *Chem. Rev.* **2005**, *105*, 3758–3772.

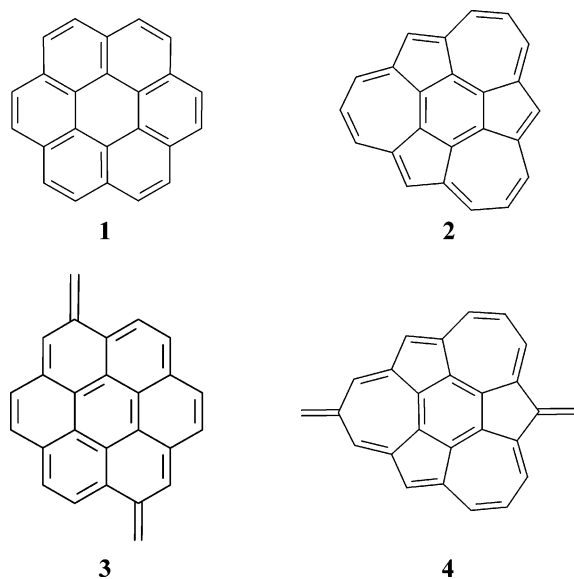
(5) Acocella, A.; Havenith, R. W. A.; Steiner, E.; Fowler, P. W.; Jenneskens, L. W. *Chem. Phys. Lett.* **2002**, *363*, 64–72.

(6) Schulman, J. M.; Disch, R. L. *J. Phys. Chem. A* **1997**, *101*, 9176–9179.

(7) Slayden, S. W.; Liebman, J. F. *Chem. Rev.* **2001**, *101*, 1541–1566.

(8) Steiner, E.; Fowler, P. W.; Jenneskens, L. W. *Angew. Chem., Int. Ed.* **2001**, *40*, 362–366.

CHART 1



From the formal point of view, this system may be represented by 20 Kekulé structures or by a set of three mobile Clar sextets, as shown in Figure 1a.<sup>10b</sup>

An aromatic sextet is defined by a set of six  $\pi$ -electrons localized in a single benzene-like ring separated from adjacent rings by formal C–C single bonds. According to Clar's rule,<sup>10b</sup> the Kekulé structure with the largest number of disjoint aromatic  $\pi$ -sextets will be the most important for the description of the properties of a given polycyclic hydrocarbon. In the case of coronene, symmetrically equivalent combinations of  $\pi$ -sextets can be written.<sup>11</sup> Coronene is not a totally resonant hydrocarbon,<sup>12</sup> however, because any one Kekulé structure leaves some carbon atoms outside sextet rings. However, Clar proposed<sup>10</sup> that if the three sextets of coronene can migrate into the neighboring rings (as shown by arrows in Figure 1a), an extra ring current will be formed. In this way, he evoked the concept of superaromaticity<sup>10b</sup> originating from a molecular sextet-migration current.

Additional support for this concept came from Hosoya and Yamaguchi<sup>13</sup> who introduced generalized Clar structures. These are defined as valence formulas (resonance structures) of a benzenoid hydrocarbon in which one or more aromatic  $\pi$ -sextets are inscribed in nonadjacent benzene rings, so that after deletion of these benzene rings with sextets, the remaining part of the structure has a Kekulé structure.<sup>12</sup> The number of generalized Clar structures matches the number of Kekulé valence structures for simple benzenoid hydrocarbons but not for coronene.<sup>13,14</sup>

(9) (a) Aihara, J.-I. *Chem. Phys. Lett.* **2002**, *365*, 34–39. (b) Aihara, J.-I. *Chem. Phys. Lett.* **2004**, *393*, 7–11. (c) Aihara, J.-I. *Chem. Phys. Lett.* **2003**, *381*, 147–153. (d) Yoshida, M.; Osawa, E.; Aihara, J.-I. *J. Chem. Soc., Faraday Trans.* **1995**, *91*, 1563–1565. (e) Aihara, J.-I. *J. Phys. Chem. A* **2003**, *107*, 11553–11557. (f) Aihara, J.-I.; Tamaribuchi, T. *J. Math. Chem.* **1996**, *19*, 231–239. (g) Aihara, J.-I. *J. Phys. Chem.* **1994**, *98*, 9772–9776. (h) Aihara, J.-I. *J. Am. Chem. Soc.* **1992**, *114*, 865–868.

(10) (a) Clar, E.; Sanigök, Ü.; Zander, M. *Tetrahedron* **1968**, *24*, 2817–2823. (b) Clar, E. *The Aromatic Sextet*; J. Wiley & Sons: London, 1972. (c) Gutman, I.; Cyvin, S. J. *Introduction to the Theory of Benzenoid Hydrocarbons*; Springer-Verlag: New York, **1989**. (d) Aihara, J.-I. *Bull. Chem. Soc. Jpn.* **1993**, *66*, 57–60.

(11) Suresh, C. H.; Gadre, S. R. *J. Org. Chem.* **1999**, *64*, 2505–2512.

(12) Randić, M. *Chem. Rev.* **2003**, *103*, 3449–3605.

(13) (a) Hosoya, H.; Yamaguchi, T. *Tetrahedron Lett.* **1975**, 4659–4662.

(b) Hosoya, H. *Top. Curr. Chem.* **1990**, *153*, 255–273.

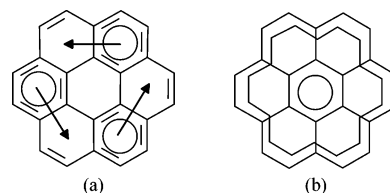
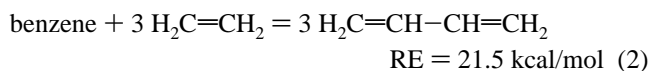
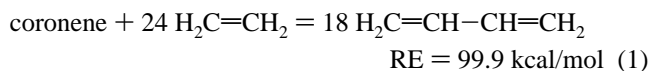


**FIGURE 1.** (a) Clar  $\pi$ -electron sextets in coronene. The arrows indicate sextet-migration. (b) Coronene seen as [18]annulene circumscribing a central benzene ring.

For coronene, equality of the counts can be maintained if an additional Clar-like structure including the 18-membered cycle around the perimeter<sup>15</sup> is taken into account (see Figure 1b). Even though the presence of such a large conjugated circuit makes little contribution to molecular resonance energy (RE),<sup>12</sup> coronene depicted as an [18]annulene circumscribing a central benzene ring has been believed to be superaromatic.<sup>10b</sup>

## Results and Discussion

Coronene has enhanced aromatic character compared to some other polycyclic hydrocarbons (e.g., naphthalene and anthracene).<sup>6</sup> Early estimates of the RE based on a topological approach<sup>16</sup> and a more recent estimate based on simple isodesmic reactions<sup>17</sup> indicate that the RE per  $\pi$ -electron (REPE) is somewhat higher for coronene than for benzene (4.2 vs 3.6 kcal/mol):



It should be noted that factors such as unbalanced strain, changes of hybridization, and other effects that do not originate from cyclic  $\pi$ -electron delocalization may all be sources of a substantial error in this case.<sup>17,18</sup> The isodesmic reaction presented above should be treated with caution, because a similar reaction for pyrene gives an REPE = 3.7 kcal/mol, and pyrene is not usually considered to be more aromatic than benzene.

Although RE considerations could be taken to indicate some enhanced aromaticity for coronene, an analysis based on geometry and magnetic properties appears to rule this out. The bond lengths in the [18]annulene perimeter show significant alternation (1.377 and 1.421 Å at the MP2/6-31G\* level) resulting in an appreciably smaller value of the geometry-based harmonic oscillator model of aromaticity (HOMA) descriptor of cyclic  $\pi$ -electron delocalization for this cycle (0.800 vs 1.0 for benzene),<sup>19</sup> while the hub bond lengths are significantly elongated (1.424 Å) implying even lower aromaticity of this fragment (HOMA = 0.662).

This difference in local aromaticity<sup>20</sup> is consistent with the conventional interpretation of NICS<sup>21</sup> values. These may be calculated at a height of 1 Å above the centers of outer and

(14) (a) Ohkami, N.; Hosoya, H. *Theor. Chim. Acta* **1983**, *64*, 153–170. (b) Wenchen, H.; Wenjie, H. *Theor. Chim. Acta* **1985**, *68*, 301–313. (c) Wenjie, H.; Wenchen, H. *Theor. Chim. Acta* **1986**, *70*, 43–51. (d) Ohkami, N. *J. Math. Chem.* **1990**, *5*, 23–42.

(15) Zhang, F.; Chen, R. S. *MATCH* **1986**, *19*, 179–188.

(16) Randić, M.; Guo, X. F. *New J. Chem.* **1999**, *23*, 251–260.

(17) See ref 7, p 1551.

(18) Cyrański, M. K. *Chem. Rev.* **2005**, *105*, 3773–3811.

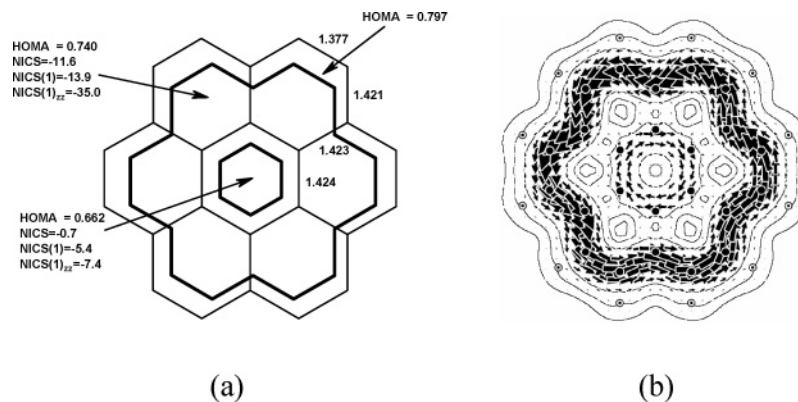


**FIGURE 2.** (a) Bond lengths and the aromaticity descriptors: HOMA, NICS, NICS(1) (calculated 1 Å above the molecular plane), and NICS(1)<sub>zz</sub> (the component of NICS(1) corresponding to the principal axis perpendicular to the ring plane) for fragments of coronene. (b) Map of π-current-density in coronene. Diatropic and paratropic circulations are shown anticlockwise and clockwise, respectively.

central rings (NICS(1) = -13.9 and -5.4 ppm, respectively, (Figure 2a)), in the plane (NICS(0)), or taken as components of NICS(1) in the direction of the magnetic field (NICS(1)<sub>zz</sub>); all are listed in Figure 2 and all give essentially the same type of information.

However, the more-detailed information available from a full current-density map, which is calculated in the ipsocentric approach, shows the danger in interpreting NICS values literally as indicators of local circulation. While the (still diatropic) -5.4 ppm plausibly might be taken to indicate a paratropic or reduced diatropic local ring current, the outer ring value of -13.9 ppm is not signaling a local circulation at all; it arises essentially from the strong flow through the outside portion of each ring (Figure 2b). Counter circulation of “rim and hub” currents is characteristic of the [n]circulenes. It follows from their characteristic frontier-orbital structure<sup>5</sup> and depends on the strength of coupling between inner and outer circuits.<sup>22</sup> It is always safer to have access to the map itself. Full sets of current-density maps can always be integrated to yield NICS and total susceptibility values, but retrieval of the rich detail of the map from the integrated properties is fraught with difficulty in all but the simplest cases.<sup>23</sup>

The rim and hub currents calculated in the ipsocentric approach clearly contradict the predictions based on the so-

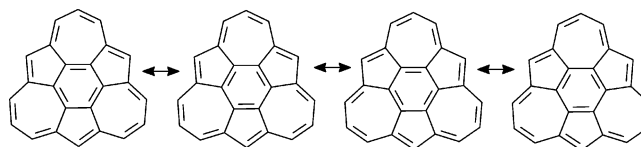


**FIGURE 3.** The four Kekulé structures of isocoronene.

called “[n]annulene-within-an-[m]annulene” model.<sup>24</sup> In accordance to this model, coronene can be represented by two decoupled monocyclic  $[4n + 2]$  π-electron annulenes. Clearly, coronene cannot be considered to be superaromatic. Before dismissing the superaromaticity concept, one important question should be considered: if it is possible to modify the ring of rings to make the π-electron structure more efficiently (super) delocalized.

Isocoronene (**2**) ([7,5,7,5,7,5]-isocoronene or [7,5,7,5,7,5:6]-circulene) is a valence isomer of coronene with the central benzene ring surrounded by three azulenes instead of naphthalenes. This molecule has only four Kekulé structures, and all have fixed formal single bonds isolating the perimeter 18-membered super-ring from the central six-membered unit (Figure 3). Although isocoronene is significantly less stable (by ca. 105 kcal/mol at the MP2/6-31G\* level) than the parent coronene, this system is not chemically unrealistic, and its carbon skeleton recently has been considered as a possible native defect in carbon nanotubes.<sup>25</sup> Moreover, this geometrical arrangement corresponds to a local minimum on the potential energy surface.

Strong π-electron delocalization in **2** is documented by the magnetic-field-induced current-density map (Figure 4b), calculated within the ipsocentric approach.<sup>26</sup> The pattern of π-electron currents in isocoronene is simpler than in coronene. Isocoronene shows a clear diatropic circulation on the perimeter reinforced by a weak central circulation in the same sense instead of the paratropic central circulation of coronene. The perimeter current in **2** is more intense than in **1**. An estimate of current strength is  $j_{\max}$ , which is the maximum magnitude of the current-density per unit inducing magnetic field taken over

(19) (a) Krygowski, T. M. *J. Chem. Inf. Comput. Sci.* **1993**, *33*, 70–78. (b) Krygowski, T. M.; Cyrański, M. *Tetrahedron* **1996**, *52*, 1713–1722. (c) Krygowski, T. M.; Cyrański, M. K. *Chem. Rev.* **2001**, *101*, 1385–1419. HOMA is defined as follows:  $\text{HOMA} = 1 - \alpha/N \sum (R_{\text{opt}} - R_i)^2$ , where  $N$  is the number of bonds taken into the summation;  $\alpha$  is an empirical constant fixed to give HOMA = 0 for a model nonaromatic system and HOMA = 1 for a system with all bonds equal to an optimal value  $R_{\text{opt}}$  that are assumed to be realized for fully aromatic systems; and  $R_i$  stands for a running bond length. Note that the approximate way of estimating  $R_{\text{opt}}$  leads to values of HOMA for benzene that are not exactly equal to 1.00 but slightly less depending on bond lengths used for calculations.

(20) Krygowski, T. M.; Cyrański, M.; Ciesielski, A.; Świrski, B.; Leszczyński, P. *J. Chem. Inf. Comput. Sci.* **1996**, *36*, 1135–1141.

(21) (a) Schleyer, P. v. R.; Maerker, C.; Dransfeld, A.; Jiao, H.; van Eikema Hommes, N. J. R. *J. Am. Chem. Soc.* **1996**, *118*, 6317–6318. (b) Chen, Z.; Wannere, C. S.; Corminboeuf, C.; Puchta, R.; Schleyer, P. v. R. *Chem. Rev.* **2005**, *105*, 3842–3888. NICS is defined as the negative value of the absolute shielding computed at the geometric center of a ring system. Now, it is also calculated at other points, inside, or around molecules. The NICS denoted as NICS(1) is calculated 1 Å above the center, NICS(1)<sub>zz</sub> is perpendicular to the plane of the ring component of NICS(1) tensor. Rings with negative NICS values qualify as aromatic and the more negative the NICS values, the more aromatic are the rings.

(22) Ege, G.; Vogler, H. *Theor. Chim. Acta* **1972**, *26*, 55–65.

(23) Steiner, E.; Fowler, P. W. *Phys. Chem. Chem. Phys.* **2004**, *6*, 261–272.

(24) Benschafut, R.; Shabtai, E.; Rabinovitz, M.; Scott, L. T. *Eur. J. Org. Chem.* **2000**, 1091–1106.

(25) Orlikowski, D.; Nardelli, M. B.; Bernholc, J.; Roland, C. *Phys. Rev. B* **2000**, *61*, 14194–14203.

(26) (a) Fowler, P. W.; Steiner, E. *J. Phys. Chem.* **1997**, *101*, 1409–1413. (b) Fowler, P. W.; Steiner, E.; Havenith, R. W. A.; Jenneskens, L. W. *Magn. Reson. Chem.* **2004**, *42*, S68–S78.

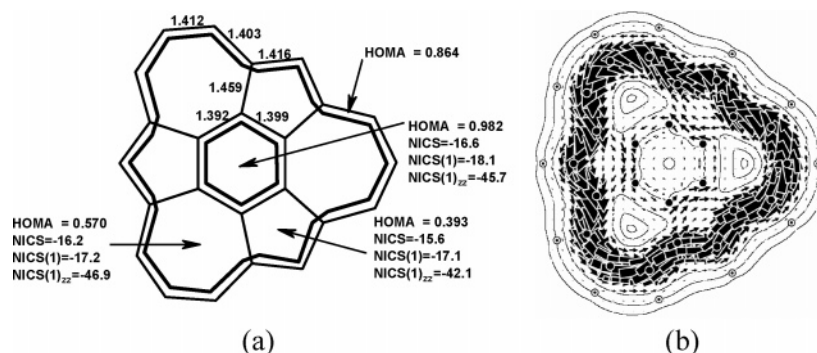


**FIGURE 4.** (a) Bond lengths and the aromaticity descriptors: HOMA, NICS, NICS(1), and NICS(1)<sub>zz</sub> for isocoronene. (b) Map of  $\pi$ -current-density in isocoronene. The NICS descriptors follow the notation used in Figure 2.

the plotting plane. For a plane 1 bohr above the nuclei, the value of  $j_{\max}$  calculated for benzene in the standard 6-31G\*\* basis is 0.08 au. In the same approach,  $j_{\max}$  for coronene is 0.11 au, and  $j_{\max}$  for isocoronene is 0.16 au or twice the standard benzene value.

If taken literally, calculated NICS(1) values indicate a high degree of local aromaticity for both inner 6- and outer 5- and 7-rings of isocoronene, although as discussed earlier, the implied local circulation does not actually exist in the current-density map, and the aromatic NICS values for 5- and 7-rings arise from the perimeter flow past rather than around the ring center. HOMA values for the perimeter 18- and central 6- circuits are compatible with the  $\pi$ -delocalization pathways indicated by the current-density map. For the 18-membered outer ring, the HOMA value is 0.864, while for the inner ring, it indicates almost the same extent of  $\pi$ -electron delocalization (HOMA = 0.982) as in the case of benzene. The low values of the local HOMA indices for the 5- and 7-rings are caused by the near single-bond character of the spoke bonds connecting the rim and hub of isocoronene (these bonds are of almost the same length as the central bond in 1,3-butadiene<sup>27</sup>).

An advantage of the ipsocentric approach to the calculation of current-density is that the total response of the molecule has a ready partition into physically nonredundant contributions from individual molecular orbitals.<sup>28</sup> Each contribution arises from a virtual excitation from an occupied to an unoccupied orbital and obeys symmetry selection rules: diatropic currents arise from translationally allowed node-increasing excitations and paratropic currents from rotationally allowed node-conserving excitations. Within this framework, just four HOMO electrons out of the 24  $\pi$ -electrons of coronene give rise to the overall pattern of current-density with the  $E_{2u} \rightarrow E_{1g}$  HOMO–LUMO excitations giving rise to the diatropic perimeter current and the  $E_{2u} \rightarrow E_{2u}$  HOMO–LUMO + 1 excitations giving the weaker paratropic current (Figure 5a). The HOMO–LUMO excitation corresponds to an increase from four to five angular nodes on the perimeter, and the HOMO–LUMO + 1 excitations preserves the node count of 2 in the inner 6-ring. In isocoronene, the current map is similarly dominated by the four HOMO electrons. The HOMO–LUMO excitation is  $E'' \rightarrow E''$  (Figure 5b) and, therefore, formally both translationally and rotationally allowed. Examination of the nodal patterns shows that both HOMO and LUMO are concentrated on the perimeter of **2**, which is where the excitation increases the angular-node count

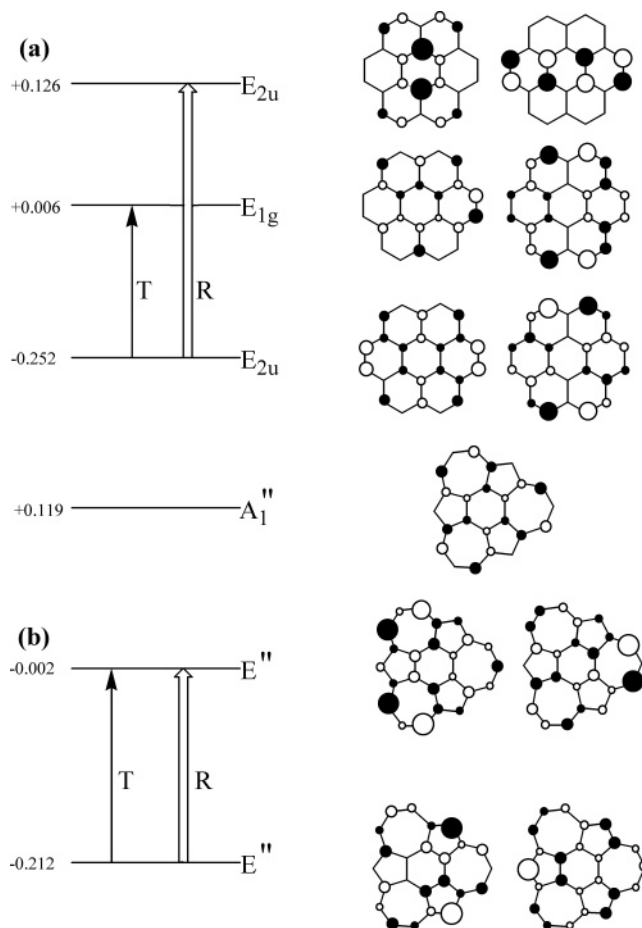


**FIGURE 5.** Schematic frontier-orbital energy level diagram for (a) coronene and (b) isocoronene that shows the HOMO, LUMO, and LUMO+1 levels of the  $\pi$  system and the corresponding orbitals and illustrates the translationally (T) and rotationally (R) allowed virtual excitations between occupied and empty orbitals. The scale is orbital energies (marked in atomic units).

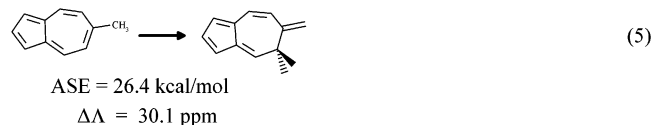
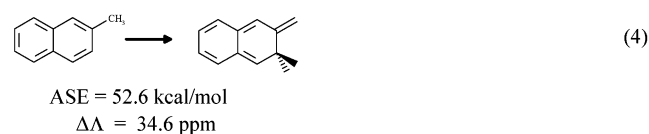
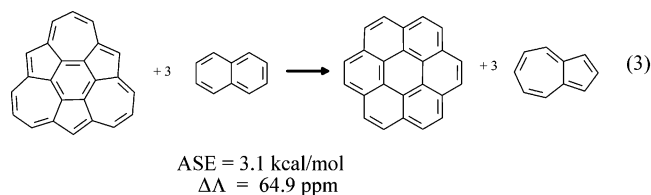
from four to five. Thus, the perimeter current in **2** has essentially the same origin as in **1** but is more intense (in line with the smaller gap) and is unopposed (in line with the lack of a suitable paratropic contribution on the central ring).

The enhanced  $\pi$ -electron delocalization of isocoronene is supported by other magnetism-based quantitative descriptors of aromaticity. Anisotropy of magnetic susceptibility,  $\Delta\chi$ , has been proposed as a criterion of aromaticity;<sup>29</sup> isocoronene has a much greater  $\Delta\chi$  (359 cgs-ppm) than coronene (247 cgs-ppm). A more

(27) Kveseth, K.; Seip, R.; Kohl, D. A. *Acta Chem. Scand.* **1980**, A34, 31–42.

(28) Steiner, E.; Fowler, P. W. *J. Phys. Chem.* **2001**, 105, 9553–9562.

widely used magnetic criterion of aromaticity is exaltation of diamagnetic susceptibility,  $\Lambda$ , defined by the difference between the mean magnetic susceptibility and a model value calculated from a scheme of local group increments. Coronene has an exaltation  $\Lambda$  of 103 cgs-ppm.<sup>8,30</sup> The mean susceptibility of isocoronene ( $-348$  cgs-ppm) is significantly larger in absolute value than that of coronene ( $-276$  cgs-ppm). An estimate of the exaltation of diamagnetic susceptibility of isocoronene may be derived from eq 3 using the magnetic susceptibilities of naphthalene and azulene ( $-96.5$  and  $-99.0$  cgs-ppm, respectively) and the corresponding exaltations (34.6 and 30.1 cgs-ppm, respectively, see eqs 4–5). As the local group increments cancel out in the balanced equation, the exaltation of isocoronene is found to exceed that of coronene by 51.4 ppm.



These equations also are used to deduce the difference in stabilization energies due to cyclic  $\pi$ -electron delocalization of coronene and isocoronene. Equation 3 balances strain between the coronene isomers by referring them to three units of azulene and naphthalene. This equation meets all homodesmotic reaction criteria,<sup>18</sup> but unlike eq 1, it does not give explicit information on the aromatic stabilization energies (ASE) of coronene or isocoronene. The isomerization evaluation method,<sup>31</sup> which is based on the difference energy between cyclically delocalized and acyclic conjugated isomers (see eqs 4–5), enables the estimation of the stabilization energies of the methylated reference molecules in eq 3, which have practically the same ASE as the respective parent systems (naphthalene and azulene). Note that the correction for syn/anti diene mismatch is not taken into account because their number is essentially the same in both reactions. From an energetic perspective, the  $\pi$ -electron delocalization in naphthalene is more efficient (ASE = 52.6 kcal/mol) than that in azulene (ASE = 26.4 kcal/mol). The stabilization of 3.1 kcal/mol deduced from eq 3 is dominated by this difference and surprisingly reveals that the ASE of isocoronene is lower by ca. 75.5 kcal/mol than the ASE of

coronene. This also is consistent with the values of REPE estimated within the Hess and Schaad approach<sup>32</sup> based on HMO calculations, which for coronene and isocoronene are equal to 0.049 and 0.012  $\beta$ , respectively. The remaining part of the 105 kcal/mol difference in the total energies between the coronene isomers (i.e., 29.5 kcal/mol) can be attributed to differential strain between the molecules. In contrast to the magnetic (and geometric) picture, the super-delocalization in isocoronene that produces the conrotary diamagnetic ring current circulation in the two cycles does not result also in an enhanced aromatic stability, and thus, the energetic criterion gives no indication of superaromaticity for isocoronene.

How do the electron (de)localization pathways change when coronene and isocoronene are perturbed? The perimeter can be perturbed by methylene groups, such as in the  $C_{2h}$  and  $C_{2v}$  – symmetric model structures (3) and (4) (see Figure 6), and these double-bonded substituents lead to efficient localization of the  $\pi$ -electronic structure.<sup>18</sup> As might be expected from simple topological considerations, the bond-fixing perturbations in coronene induce an anthracene subunit, which can be clearly distinguished by its diamagnetic ring current on the current-density map (Figure 6b). The anthracene unit supports a current that is slightly stronger than in benzene ( $j_{\max} = 0.09$  au, cf.  $j_{\max} = 0.08$  au for benzene). NICS and HOMA parameters for this fragment are comparable to those of anthracene,<sup>33</sup> although the NICS values are swapped between outer and central rings.

In the case of isocoronene, the localization of double bonds induced by the perturbing methylene groups destroys the diatropic perimeter current and leads instead to a diatropic current on the central 6-ring ( $\sim 80\%$  of the current in benzene itself) and paratropic circulation in the three heptagonal rings (see Figure 6e). Analysis in terms of orbital contributions shows that the heptagonal currents arise from the  $B_1 \pi$  HOMO (Figure 6d), while the central benzenoid ring current is a superposition of contributions from the full set of  $\pi$  MOs. The positive NICS(1) values for the 7-rings are derived from their paratropic local currents, whereas the negative values for the 5-rings are not connected to any consistent local circulation. Interestingly, NICS(1) for the central ring is only half that for the same ring in isocoronene itself, even though the current is more intense. HOMA measures are not helpful in this system because of the complex pattern of bond lengths.

## Computational Details

Geometries were initially computed at the B3LYP/6-31G\* level of theory.<sup>34</sup> All species corresponded to minima at the B3LYP/6-31G\* level with no imaginary frequencies. The systems were

(32) (a) Hess, B. A.; Schaad, L. J. *J. Am. Chem. Soc.* **1971**, *93*, 305–310. (b) for review see: Schaad, L. J.; Hess, B. A., Jr. *Chem. Rev.* **2001**, *101*, 1465–1476.

(33) (a) Cyrański, M. K.; Stępień, B. T.; Krygowski, T. M. *Tetrahedron* **2000**, *56*, 9663–9667. (b) Schleyer, P. v. R.; Manoharan, M.; Jiao, H.; Stahl, F. *Org. Lett.* **2001**, *3*, 3643–3646.

(34) Frisch, M. J.; Trucks, G. W.; Schlegel, H. B.; Scuseria, G. E.; Robb, M. A.; Cheeseman, J. R.; Zakrzewski, V. G.; Montgomery, J. A.; Stratmann, R. E.; Burant, J. C.; Dapprich, S.; Millam, J. M.; Daniels, A. D.; Kudin, K. N.; Strain, M. C.; Farkas, O.; Tomasi, J.; Barone, V.; Cossi, M.; Cammi, R.; Mennucci, B.; Pomelli, C.; Adamo, C.; Clifford, S.; Ochterski, J.; Petersson, G. A.; Ayala, P. Y.; Cui, Q.; Morokuma, K.; Malick, D. K.; Rabuck, A. D.; Raghavachari, K.; Foresman, J. B.; Cioslowski, J.; Ortiz, J. V.; Stefanov, B. B.; Liu, G.; Liashenko, A.; Piskorz, P.; Komaromi, I.; Gomperts, R.; Martin, R. L.; Fox, D. J.; Keith, T.; Al-Laham, M. A.; Peng, C. Y.; Nanayakkara, A.; Gonzalez, C.; Challacombe, M.; Gill, P. M. W.; Johnson, B. G.; Chen, W.; Wong, M. W.; Andres, J. L.; Head-Gordon, M.; Replogle, E. S.; Pople, J. A. *Gaussian 98*, Revision A.7; Gaussian, Inc.: Pittsburgh, PA, 1998.

(29) (a) Benson, R. C.; Flygare, W. H. *J. Am. Chem. Soc.* **1970**, *92*, 7523–7529. (b) Benson, R. C.; Flygare, W. H.; Beak, P. *J. Am. Chem. Soc.* **1971**, *93*, 5591–5593. (c) Fleischer, U.; Kutzelnigg, W.; Lazzarotti, P.; Mühlenkamp, V. *J. Am. Chem. Soc.* **1994**, *116*, 5298–5306. (d) Lazzarotti, P. *Phys. Chem. Chem. Phys.* **2004**, *6*, 217–223. (e) Lazzarotti, P. *Prog. Nucl. Magn. Reson. Spectrosc.* **2000**, *36*, 1–88. (f) Schleyer, P. v. R.; Jiao, H. *Pure Appl. Chem.* **1996**, *68*, 209–218.

(30) Dauben, H. J.; Wilson, J. D.; Laity, J. L. In *Nonbenzenoid Aromatics*; Snyder, J. P., Ed.; Academic Press: New York, 1971; Vol. 2, pp 167–206.

(31) Schleyer, P. v. R.; Pühlhofer, F. *Org. Lett.* **2002**, *4*, 2873–2876.

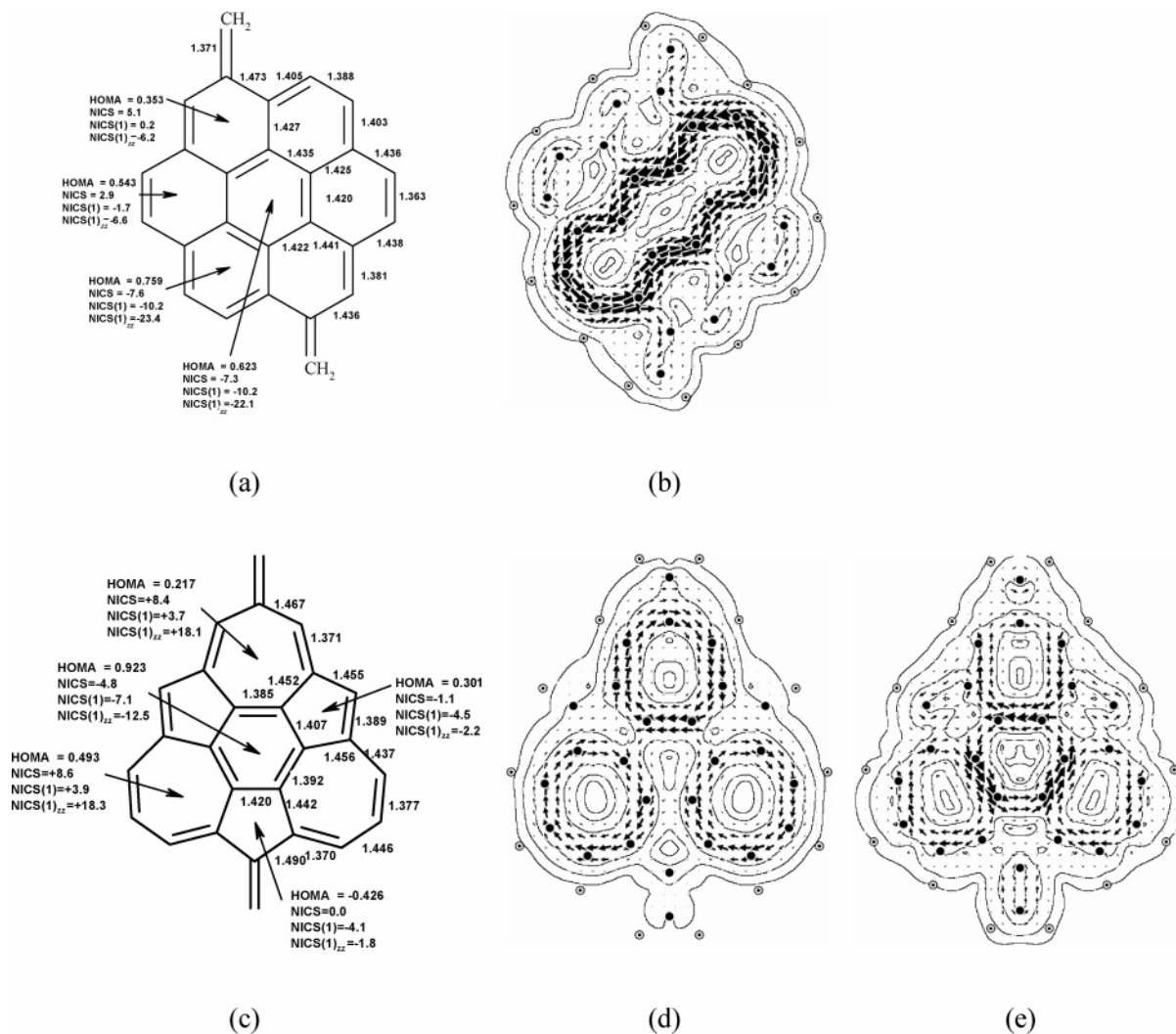


**FIGURE 6.** (a) Bond lengths and the aromaticity descriptors: HOMA, NICS, NICS(1), and NICS(1)<sub>zz</sub> for fragments of dimethylene-substituted coronene. (b) Map of  $\pi$ -current-density in the coronene derivative **3**. (c) Bond lengths and the aromaticity descriptors: HOMA, NICS, NICS(1), and NICS(1)<sub>zz</sub> for fragments of a dimethylene-substituted isocoronene **4**. Maps of  $\pi$ -current-density in the isocoronene derivative: (d) contribution from the B<sub>1</sub> HOMO; (e) sum of contributions from all orbitals of  $\pi$  symmetry.

reoptimized at the MP2(fc)/6-31G\* level of theory. CSGT calculations employed MP2(fc)/6-31G\* optimized geometries, and the HF/6-311G\*\* basis set was selected for the calculation of the exaltation of magnetic susceptibility. The GIAO/HF/6-311G\*\* method was used for the NICS calculations. The HOMA values were based on molecular geometries optimized at the MP2(fc)/6-31G\* level. All current-density maps were calculated at the ipso-centric 6-31G\*\*/CTOCD-DZ level using the SYSMO<sup>35</sup> package.

**Acknowledgment.** We are grateful to the referees for their thoughtful comments, which helped us to improve the paper,

(35) Lazzaretto, P.; Zanasi, R. SYSMO package University of Modena, 1980 (additional routines by Steiner, E.; Fowler, P. W.; Havenith R. W. A.; Soncini, A.).

and for providing the REPE values of coronene and isocoronene. The Interdisciplinary Centre for Mathematical and Computational Modelling (Warsaw) is kindly acknowledged for computational facilities. P.W.F. is supported by a Royal Society/Wolfson Research Merit Award. M.L. thanks EPSRC for financial support.

**Supporting Information Available:** Absolute electronic energies at MP2(fc)/6-31G\* (in hartree) and Cartesian coordinates at MP2(fc)/6-31G\*, magnetic susceptibilities (in cgs-ppm) and anisotropies of magnetic susceptibility calculated with use of CSGT method at HF/6-311G\*\* for the molecules studied. This material is available free of charge via the Internet at <http://pubs.acs.org>.

JO060898W